Preprint HU-TFT-93-43

THE GROWTH OF BUBBLES IN COSMOLOGICAL PHASE TRANSITIONS

J. Ignatius[*,b], K. Kajantie[†,a], H. Kurki-Suonio[‡,b] and M. Laine[§,a]

[a]*Department of Theoretical Physics and*
[b]*Research Institute for Theoretical Physics,*
P.O. Box 9, 00014 University of Helsinki, Finland

27 September 1993

Abstract

We study how bubbles grow after the initial nucleation event in generic first-order cosmological phase transitions characterised by the values of latent heat L, interface tension σ and correlation length ξ, and driven by a scalar order parameter ϕ. Equations coupling $\phi(t, \mathbf{x})$ and the fluid variables $\mathbf{v}(t, \mathbf{x})$, $T(t, \mathbf{x})$ and depending on a dissipative constant Γ are derived and solved numerically in the 1+1 dimensional case starting from a slightly deformed critical bubble configuration $\phi(0, \mathbf{x})$. Parameters L, σ, ξ corresponding to QCD and electroweak phase transitions are chosen and the whole history of the bubble with formation of combustion and shock fronts is computed as a function of Γ. Both deflagrations and detonations can appear depending on the values of the parameters. Reheating due to collisions of bubbles is also computed.

PACS numbers: 98.80.Cq, 11.10.Lm, 64.60.-i

[*]email: ignatius@phcu.helsinki.fi
[†]email: kajantie@phcu.helsinki.fi
[‡]email: hkurkisu@pcu.helsinki.fi
[§]email: mlaine@phcu.helsinki.fi

1 Introduction

The bubble nucleation in cosmological first-order phase transitions as well as the propagation and stability of planar interfaces have been discussed extensively in the literature [1]–[19]. The purpose of this paper is to join these two ends of the life of a bubble by giving a dynamical model which describes the entire history of the bubble from the initial configuration via initial acceleration into a large bubble growing with constant velocity.

The stage for the events in this paper is the cosmic fluid with a first-order phase transition at $T = T_c$ — in practice either the QCD or the electroweak (EW) phase transition. For physical quark masses there is no symmetry associated with the former one and its order is not definitely confirmed [20]. The latter is a symmetry breaking transition and, at least for not too large Higgs masses, it is of first order both on the basis of perturbative [21]–[26] and nonperturbative lattice Monte Carlo [27]–[29] work. Inflationary transitions are essentially vacuum ones and the considerations here do not apply.

The main quantity characterizing the cosmic fluid is its energy-momentum tensor $T^{\mu\nu} = (\epsilon + p)u^\mu u^\nu - pg^{\mu\nu}$. The first-order nature implies that there are two phases, a high temperature phase (symmetric, quark-gluon plasma phase) with pressure $p_q(T)$ and a low temperature phase (broken symmetry, hadron phase) with pressure $p_h(T)$, which can coexist at T_c: $p_q(T_c) = p_h(T_c)$ but $p'_q(T_c) > p'_h(T_c)$. We shall describe the transition by a scalar order parameter field $\phi(t, \mathbf{x})$. This is obvious for a symmetry breaking transition, but we shall use the same description also if no symmetry is involved: the order parameter could then be, for example, the energy or entropy density. The bubbles are configurations of $\phi(t, \mathbf{x})$.

The problem now is to derive equations of motion for the total cosmic fluid – order parameter field system. We carry this out in analogy with the reheating problem in inflation [30,31]. The total energy momentum tensor of the system is conserved ($\partial_\nu T^{\mu\nu} = 0$) but those of the fluid and order parameter field subsystems are not. Physically, entropy produced at the bubble interface couples the behavior of ϕ with the fluid. The strength of this coupling is described by a dissipative constant Γ. It has been related by a fluctuation-dissipation formula to equilibrium averages in refs. [32,33], but we use Γ as a phenomenological parameter. Estimates for it in the EW theory have been given in refs. [11,34].

Given the equations of motion one can solve them numerically and study how bubbles corresponding to given initial supercooling (which follows from nucleation analysis), given parameters of the transition (latent heat, interface tension, correlation lengths), and given dissipative constant Γ evolve. Collisions of bubbles can be similarly studied. In this first discussion we shall solve the equations in 1+1 (one time, one space) dimensions, which contains the main qualitative features. For complete quantitative results one must go to 1+2 or 1+3 dimensions.

The initial stages of bubble growth have also been computed by integrating spherically symmetric 1+3 dimensional hydrodynamic equations in ref. [35]. The velocity is taken as a free parameter, effectively parametrised by the magnitude of energy flux. Our work differs in one essential aspect from this: the dissipative constant Γ is at least in principle calculable from the theory.

The paper is organized as follows. In Section 2 we introduce our model for the first-order phase transitions. In Section 3 we review the general hydrodynamic conditions for the bubbles, and describe the two kinds of solutions, detonations and deflagrations. In Section 4 we describe our results for different time-dependent phenomena like the initial stages of bubble formation, the sharpening of shock fronts and the collisions between expanding bubbles. In Section 5 we give an account of the different steady-state variables for deflagrations (temperatures and velocities) as a function of Γ. The conclusions are in Section 6.

2 Equations of motion for the cosmic fluid and the order parameter field

The system we consider contains the cosmic fluid which has supercooled in the metastable high T phase (call it by convention q) to some temperature T_f. At this temperature nucleation of bubbles of the low T phase (call it by convention h) becomes sufficiently frequent for the phase transition to effectively take place. We shall first define the quantities appearing in the equations of motion.

The bubbles are defined as configurations $\phi(t, \mathbf{x})$ of a scalar order parameter ϕ. The (meta)stable states of the system are defined by the minima of the effective potential $V(\phi, T)$ of the order parameter ϕ. The equations will be formulated for a general V, but for numerical calculations we shall use a quartic parametrisation [3,14]:

$$V(\phi, T) = \frac{1}{2}\gamma(T^2 - T_0^2)\phi^2 - \frac{1}{3}\alpha T\phi^3 + \frac{1}{4}\lambda\phi^4. \tag{1}$$

The full functional form of the ring summation improved effective potential [22]–[26] deviates somewhat from this, and even more does the effective potential containing nonperturbative effects [29]. The methods developed here can be straightforwardly extended to these improved potentials.

The physical quantities corresponding to the parameters α, γ, λ and T_0 in eq. (1) are the latent heat L, the interface tension σ, the critical temperature T_c and the correlation length $\xi(T_c) \equiv \xi_c$ [15]. The quartic parametrisation in eq. (1) implies that the correlation lengths in the two phases at T_c are equal, but actually they are different [29].

The primary physical quantities characterizing the transition are T_c, L, σ and ξ_c, and given these, we can always solve for the parameters α, γ, λ and T_0 in eq. (1). In this way we can use eq. (1) also for QCD. Its use for a symmetry breaking transition is, of course, obvious.

For the equation of state of the system we shall take

$$p_q(T) = aT^4 \qquad p_h(T) = aT^4 + B(T), \tag{2}$$

where $B(T) = -V(\phi_{\min}, T)$ is the difference between the free energy densities of the symmetric and the broken symmetry phases. The number of effective degrees of freedom of the high temperature phase is denoted by g_*, and $a \equiv (\pi^2/90)g_*$.

Summarizing, our dynamical variables are the four-velocity of the fluid $u^\mu(t, \mathbf{x})$, the scalar field $\phi(t, \mathbf{x})$ and the local temperature $T(t, \mathbf{x})$. We use the notations $w_r = 4aT^4$ and $p_r = aT^4$ for the pure radiative enthalpy and pressure, respectively.

To motivate and to write down the equations of motion we first write the effective potential of eq. (1) in two parts:

$$V(\phi, T) = \underbrace{-\frac{1}{2}\gamma T_0^2\phi^2 + \frac{1}{4}\lambda\phi^4}_{V_0(\phi)} + \underbrace{\frac{1}{2}\gamma T^2\phi^2 - \frac{1}{3}\alpha T\phi^3}_{V_1(\phi,T)} \ . \tag{3}$$

The part $V_0(\phi)$ is related strictly to the scalar field, whereas the part $V_1(\phi, T)$ includes the interaction of the field with the thermal bath. The total energy-momentum tensor is

$$\begin{aligned} T^{\mu\nu} \ &= \ \partial^\mu\phi\partial^\nu\phi - g^{\mu\nu}[\frac{1}{2}\partial_\alpha\phi\partial^\alpha\phi - V_0(\phi)] && (4)\\ &\quad + [w_r - T\frac{\partial V_1(\phi, T)}{\partial T}]u^\mu u^\nu - g^{\mu\nu}[p_r - V_1(\phi, T)] \ , && (5) \end{aligned}$$

and it is of course conserved:

$$\partial_\mu T^{\mu\nu} = 0 \ . \tag{6}$$

The idea now is to bring in a dissipative term which acts as a friction force for the scalar field and accounts for the entropy production at the phase transition surface. This is done by splitting eq. (6) into two:

$$0 = \partial_\mu T^{\mu\nu} = [\partial_\mu T^{\mu\nu}]_\phi + [\partial_\mu T^{\mu\nu}]_{\rm rad} = \delta^\nu - \delta^\nu \ . \tag{7}$$

The form of the Lorentz-covariant dissipative term δ^ν is adopted from the context of inflation [30,31]. Because of the temperature dependence of the effective potential, the choice of the terms $[\partial_\mu T^{\mu\nu}]_\phi$ and $[\partial_\mu T^{\mu\nu}]_{\rm rad}$ in eq. (7) is not unique. It seems most natural to make the splitting in the following way:

$$\begin{aligned}
&\partial_\mu\{\partial^\mu\phi\partial^\nu\phi - g^{\mu\nu}[\tfrac{1}{2}\partial_\alpha\phi\partial^\alpha\phi - V_0(\phi)]\} + \tfrac{\partial V_1(\phi,T)}{\partial\phi}\partial^\nu\phi = -\tfrac{1}{\Gamma}u^\mu\partial_\mu\phi\partial^\nu\phi \\
&\partial_\mu\{[w_r - T\tfrac{\partial V_1(\phi,T)}{\partial T}]u^\mu u^\nu - g^{\mu\nu}p_r\} + \tfrac{\partial V_1(\phi,T)}{\partial T}\partial^\nu T = +\tfrac{1}{\Gamma}u^\mu\partial_\mu\phi\partial^\nu\phi
\end{aligned} \tag{8}$$

After all, if $V_1(\phi,T)$ could have been written in the form $V_1(\phi,T) = V_\phi(\phi) + V_T(T)$, there would be no ambiguity in the splitting, and exactly eqs. (8) would result. Our final equations are then

$$\begin{aligned}
&\partial_\mu\partial^\mu\phi + \tfrac{\partial V}{\partial\phi} = -\tfrac{1}{\Gamma}u^\mu\partial_\mu\phi \\
&\partial_\mu\{[w_r - T\tfrac{\partial V}{\partial T}]u^\mu u^\nu - g^{\mu\nu}[p_r - V]\} = (\tfrac{1}{\Gamma}u^\mu\partial_\mu\phi + \tfrac{\partial V}{\partial\phi})\partial^\nu\phi \ ,
\end{aligned} \tag{9}$$

where a common factor has been dropped.

Contracting both sides of the lower of eqs. (9) with the fluid four-velocity u_ν one gets

$$T\partial_\mu[(s_r - \frac{\partial V}{\partial T})u^\mu] = \frac{1}{\Gamma}(u^\mu\partial_\mu\phi)^2 \ , \tag{10}$$

where $s_r = 4aT^3$ is the radiative entropy and $-\frac{\partial V}{\partial T}$ the entropy associated with the order parameter. This equation relates entropy production and the gradients of ϕ via the constant Γ. Note that in a weak coupling theory [11,34] $1/\Gamma \sim 1/\tau_c \sim nv\sigma \sim g^2T$.

In this paper we study eqs. (9) in 1+1 dimensions, which corresponds to planar symmetry. While this is a drastic simplification, it nevertheless should correctly describe the late stages of the bubble growth in the 1+3 dimensional world. Planar symmetry also allows us to compare our results with analytical calculations.

In the planar-symmetry case it is also illuminating to write down the equations for the steady-state solution. At large times the system should evolve to a solution containing a combustion front moving at constant velocity. In the rest frame of the front all time derivatives then vanish and eqs. (9) become

$$\phi''(x) = \frac{\partial V}{\partial\phi} + \frac{v\gamma}{\Gamma}\phi'(x) \tag{11}$$

$$(4aT^4 - T\frac{\partial V}{\partial T})\gamma^2 v = \text{const.} \tag{12}$$

$$(4aT^4 - T\frac{\partial V}{\partial T})\gamma^2 v^2 + aT^4 + \frac{1}{2}\phi'(x)^2 - V = \text{const.} \tag{13}$$

Eqs. (12) and (13) actually also follow from the steady-state energy-momentum conservation:

$$\partial_x T^{x\mu} = 0 \ . \tag{14}$$

Similarly, the entropy production equation (10) becomes

$$T\frac{d}{dx}[(s_r-\frac{\partial V}{\partial T})\gamma v]=\frac{1}{\Gamma}\gamma^2v^2[\phi'(x)]^2. \tag{15}$$

The standard analysis of deflagration and detonation bubbles [7] is a study of what solutions eqs. (12), (13) allow. For given initial T_f this leaves a one parameter family of solutions. For detonations there are four quantities, T_q, v_q, T_h, v_h, constrained by two equations and by the boundary value $T_q = T_f$. For deflagrations the shock front has to be taken into account, and there are two more quantities but also two more equations. This is discussed in Section 3. Eq. (11) is the new one which gives the new physics permitting one to choose the correct solution within the one parameter family.

3 Deflagrations *vs.* detonations

There are two kinds of bubbles allowed by the hydrodynamics. These are called deflagration and detonation bubbles [7] according to the nature of the phase transition front.

Consider fluid flow in the rest frame of the phase transition front. The incoming flow velocity is denoted by v_1 and the outgoing velocity is denoted by v_2 (see fig. 1). In a deflagration the incoming flow is subsonic, $v_1 < c_s$, and the fluid is accelerated by the phase transition, $v_2 > v_1$, whereas for a detonation the opposite is true: $v_1 > c_s$ and $v_2 < v_1$. Depending on whether the outflow is sub- or supersonic, these processes are further divided into weak ($v_2 < c_s$), Jouguet ($v_2 = c_s$), and strong ($v_2 > c_s$) deflagrations, and strong ($v_2 < c_s$), Jouguet ($v_2 = c_s$), and weak ($v_2 > c_s$) detonations [5].

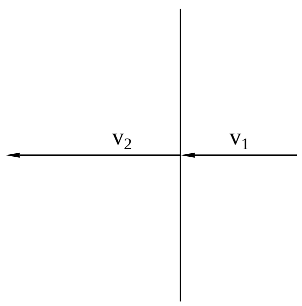

Fig. 1: The velocities in the rest frames of the phase transition and shock fronts.

Consider then the structure of the bubble in the rest frame of the ambient fluid. When the bubble has grown large enough, any memory of the initial shape

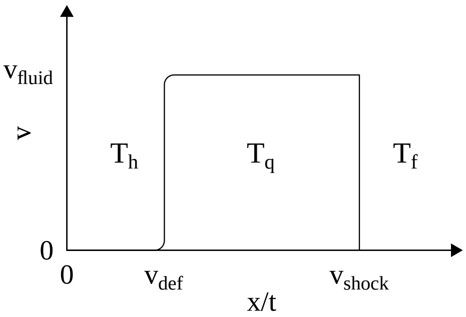

Fig. 2: Structure of a deflagration bubble.

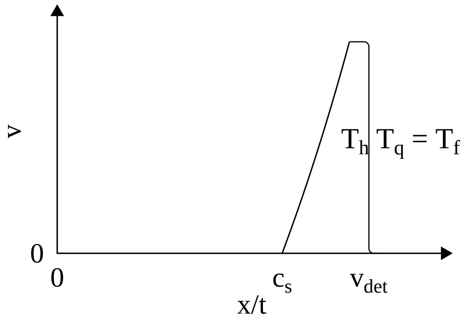

Fig. 3: Structure of a detonation bubble.

of the nucleated bubble should be lost. The bubble can then be described as a similarity solution of the hydrodynamical equations, i.e., it expands linearly with time, otherwise maintaining its shape and profile. The fluid has to be at rest both at the center of the bubble, and far away. Thus, in a deflagration bubble, the phase transition front is preceded by a shock wave which heats up the fluid and sets it moving outward. The phase transition front then brings the fluid back to rest (see fig. 2). In a detonation bubble, the fluid is at rest when it is hit by the phase transition front, which leaves the fluid flowing outward. A rarefaction wave follows, bringing the fluid at rest (see fig. 3). We denote the velocity of the phase transition front in this frame by $v_{\rm def}$ for deflagrations and by $v_{\rm det}$ for detonations. Weak deflagrations have $v_{\rm def} < c_s$, whereas for strong deflagrations $v_{\rm def} > c_s$. Detonations always have $v_{\rm det} > c_s$. We can exclude strong detonations [6], because they leave the fluid flowing too fast: no such similarity flow exists that would bring the fluid at rest at the center of the bubble [8]. For a deflagration bubble, the velocity $v_{\rm shock}$ of the shock front is also of interest. In 1+1 dimensions the fluid flows at a constant velocity $v_{\rm fluid}$ between the shock and phase transition fronts.

For deflagrations, the velocities $v_{\rm def}$, $v_{\rm fluid}$ and $v_{\rm shock}$ are related to the velocities v_1 and v_2 by the equations

$$\begin{array}{ll} v_{\rm shock} = v_1|_{\rm shock} & v_{\rm def} = v_2|_{\rm phase\ wall} \\[2ex] v_{\rm fluid} = \left.\frac{v_1-v_2}{1-v_1v_2}\right|_{\rm shock} & v_{\rm fluid} = \left.\frac{v_2-v_1}{1-v_2v_1}\right|_{\rm phase\ wall} \end{array} ,$$

where the words "shock" and "phase wall" indicate the front at which v_1 and v_2 are measured. For the phase transition front, we sometimes use the notations $v_1 = v_q$ and $v_2 = v_h$, and T_q and T_h for the temperatures of the incoming and outgoing fluids, respectively. The temperature between the fronts is then T_q and the temperature of the hadron phase is T_h (see fig. 2).

The initial condition, matter at rest in the q phase, at temperature $T_f < T_c$, and the equations of state of both phases, do not fix the rate of bubble growth ($v_{\rm def}$ or $v_{\rm det}$), or the temperature inside the bubble. For simplicity, we illustrate this with the bag equation of state[1]

$$\begin{aligned} p_h(T) &= a_h T^4 + L/4 \qquad & p_q(T) &= a_q T^4 \\ \epsilon_h(T) &= 3a_h T^4 - L/4 \qquad & \epsilon_q(T) &= 3a_q T^4 \end{aligned} \tag{16}$$

which one gets from eq. (2) by making the small-supercooling approximation

$$B(T) \sim \frac{L}{4}\left(1 - \frac{T^4}{T_c^4}\right). \tag{17}$$

Then $a_q = a$, $a_h = a - L/4T_c^4$.

The conservation of energy and momentum, and the non-negative entropy production at the phase transition front restrict the possible values of the incoming (ϵ_1) and outgoing (ϵ_2) energy densities [7] (see fig. 4). Detonations require a certain amount of supercooling. If the latent heat L is large, the required supercooling can be quite substantial, and the h matter then at a highly superheated state immediately behind the phase transition front. This has led to the conclusion that deflagrations are the more likely process in the QCD phase transition in the early universe [7].

However, if the latent heat is small, detonations require less supercooling. The nucleation temperature can be estimated [15] from

$$1 - \frac{T_f}{T_c} = \frac{A}{\sqrt{171 - 4\ln(171^{3/2}/A)}}, \tag{18}$$

where $171 = 4\ln(t_c T_c)$ and $A = \sqrt{16\pi/3}(\sigma^{3/2}/L\sqrt{T_c})$. The values of the parameters σ and L are essentially unknown, although results from lattice calculations can be employed in giving rough estimates for them. In fig. 5 we show the region in the (L, σ) parameter plane, where weak or Jouguet detonations would be allowed.

To choose among the allowed solutions (see fig. 4) the internal mechanism of the phase transition front needs to be considered. This is the purpose of our model presented in Section 2, with the additional parameter Γ, which will pick a single solution. In the next sections we turn to numerical results obtained for this model.

For the QCD phase transition we used the "**qh**" parameters

$$\begin{aligned} L &= 2 \qquad & \sigma &= 0.1 \\ \xi_c &= 1 \qquad & g_* &= 51.25 \end{aligned}$$

[1] Usually the bag constant $B = L/4$ appears on the q side, with the opposite sign. This normalization of the zero-point of energy does not affect the hydrodynamics.

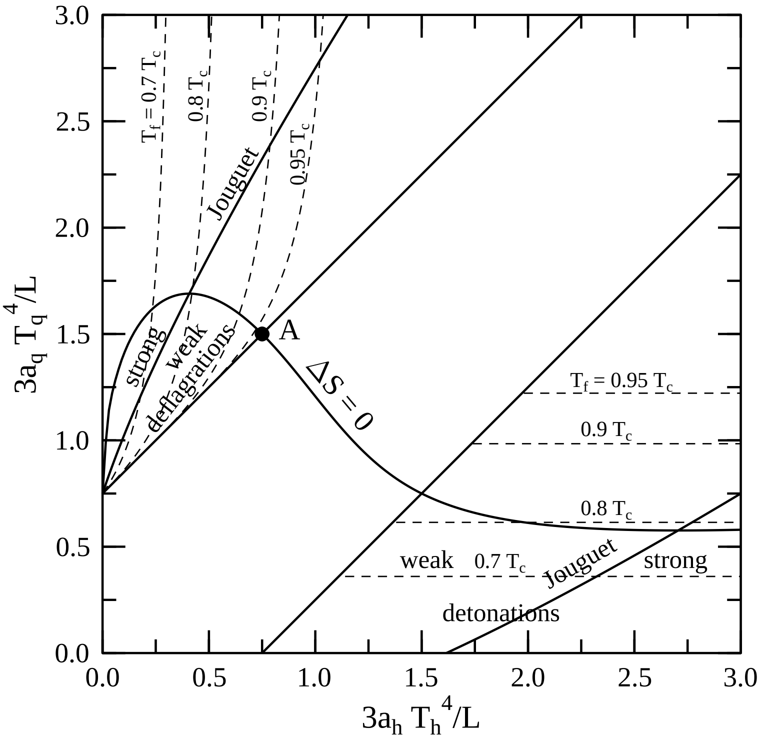

Fig. 4: The values of incoming (q) and outgoing (h) energy densities at the phase transition front, corresponding to deflagrations (upper left triangular region) and detonations (lower right). This figure is for a bag model with $r \equiv a_q/a_h = 2$. Point A corresponds to $T_q = T_h = T_c$. In deflagrations the fluid has been heated by the shock, so $T_q > T_f$, whereas for detonations $T_q = T_f$. For a given initial temperature T_f, there is a one-dimensional space of solutions, indicated by the dashed lines. The requirement of non-negative entropy production restricts the solution below the line $\Delta S = 0$. Thus, in this case, only deflagrations are allowed for $T_f = 0.9T_c$. For $T_f = 0.8T_c$, both deflagrations and weak detonations are possible. For $T_f = 0.7T_c$, Jouguet detonations are allowed, too.

Here and in the following all quantities are expressed scaled with powers of T_c to make them dimensionless: $L = L/T_c^4, \sigma = \sigma/T_c^3, \xi_c = \xi_c T_c$. From eq. (18), these parameters correspond to the nucleation temperature $T_f = 0.9943$. The values of the latent heat L and the surface tension σ are suggested by pure glue lattice Monte Carlo simulations [36,37,38]. The parameter ξ_c shows up neither when the nucleation temperature is calculated (in the thin wall approximation, eq. (18)) nor when the steady-state variables are calculated (in eqs. (30–35)). However, it determines the thickness of the phase transition surface. Because the transition is only weakly first order, the actual ξ_c might be larger than our value. Notice that in addition to strongly interacting degrees of freedom, the parameter g_* includes weakly and electromagnetically interacting degrees of freedom. Because the mean free paths of these particles are much larger than those of strongly interacting particles, these degrees of freedom are actually not active during the early stages of the phase transition [35,39]. However, since we are mostly interested in the final stationary stages of the phase

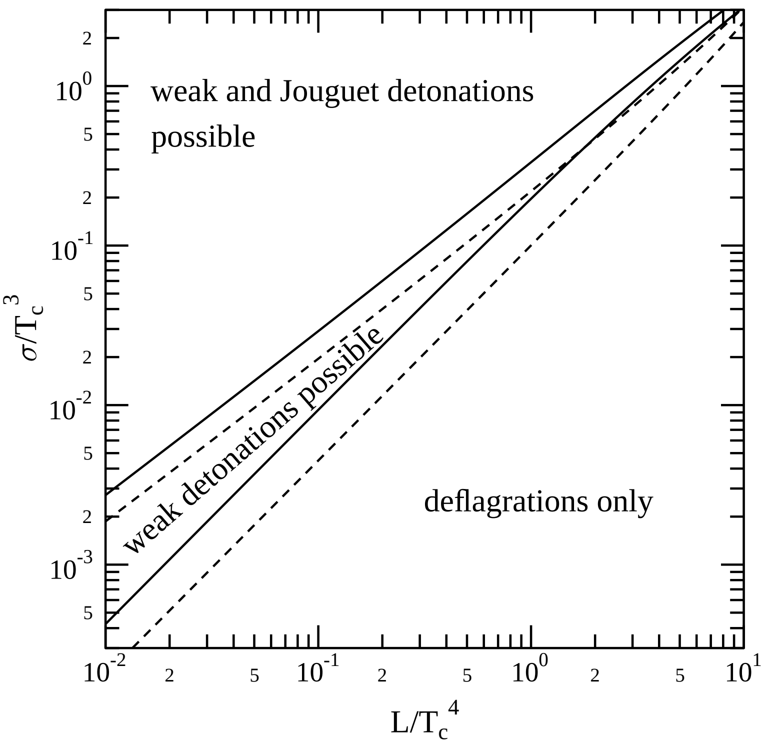

Fig. 5: For sufficiently small latent heat L, or sufficiently large surface tension σ, detonations are possible in addition to deflagrations. The precise regions in the (σ, L) plane depend on the equation of state. This figure is for a bag model with $a_q = 51.25\pi^2/90$, $a_h = a_q - L/4T_c^4$ (solid boundaries), or with $a_q = a_h + L/4T_c^4$, $a_h = 17.25\pi^2/90$ (dashed boundaries).

transition, all the degrees of freedom are included. For these parameters we expect deflagrations only (see fig. 5).

In the EW case, we assumed that $\alpha_W \approx 1/30$, $m_{\rm top} = m_W$ and $m_H \approx 40$ GeV. The small effective Higgs mass is necessary in order to allow for a generation of the baryon asymmetry. Using the improved effective potential [14] we get our "**ew**" parameters

$$\alpha = 0.0162 \qquad \gamma = 0.1309$$

$$\lambda = 0.0131 \qquad g_* = 106.75$$

This corresponds to the nucleation temperature $T_f = 0.9957$ [12].

For the above **qh** parameters the lowest temperature T_0 where the symmetric minimum $\phi = 0$ still exists is $T_0 = 0.8771$. In the **ew** case we have $T_0 = 0.9828$. That these numbers are not too low indicates that our use of the quartic effective potential $V(\phi, T)$ is justified [12, eq. (2.21)].

4 Time-dependent phenomena

To integrate eqs. (9) we wrote a simple 1+1 dimensional relativistic hydrodynamics code following Wilson [31,40]. Thus we use explicit differencing with operator splitting for the hydrodynamic equations. The code variables are ϕ, $\pi \equiv \partial_t\phi$, $E \equiv \gamma[3aT^4 + V(\phi,T) - T\frac{\partial V}{\partial T}]$, and $Z \equiv \gamma^2 v[4aT^4 - T\frac{\partial V}{\partial T}]$. The velocity v is solved from E and Z. The temperature T (for each grid point) is solved from E and ϕ using the functional form of $V(\phi,T)$. This value for T is then used in $V(\phi,T)$ for evolving ϕ. The transport terms for E and Z are handled with the FCT method [41,42].

We use reflective boundary conditions (see fig. 6). The center of the initial "bubble" of new phase is placed at one end of the grid. Allowing the moving wall to reach the other end simulates the collision with another similar bubble. The code corresponds to a planar geometry, so these are not true spherical bubbles. In this paper we study the motion of a planar phase wall.

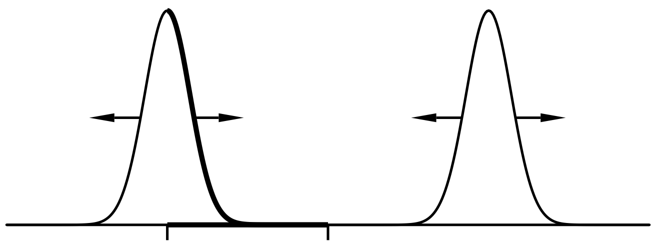

Fig. 6: The meaning of the reflective boundary conditions.

4.1 Initial conditions

Before starting the actual integration, the initial conditions have to be specified. The initial bubble has to be larger than critical to start growing, but it is not clear to what extent there is a fluctuation in the temperature associated with the fluctuation in the order parameter. Possibly the temperature is a bit higher near the critical bubble than farther away from it, because latent heat is released in the formation of the critical bubble. We can estimate typical temperature fluctuations with classical fluctuation theory [43]: for the quark matter equation of state

$$\frac{\langle(\Delta T)^2\rangle}{T^2} = \frac{1}{12aT^3V} \; . \tag{19}$$

For the **qh** case, with a radius $R_c \approx 5\xi_c$ of the critical bubble, we get $\Delta T \approx 0.005$ in units of T_c. Comparing with T_f in the previous section, this is very large. For the **ew** case we get $\Delta T \approx 0.001$ [28]. However, we think that it is most straightforward and in the spirit of the nucleation calculation (e.g. in ref. [12]) to assume that the temperature inside the initial bubble is just T_f. What is most important, the details of the initial bubble have no effect on the final steady-state configuration and the asymptotic variables T_q, T_h, v_{shock}, v_{fluid} and v_{def} (or v_{det}), if only the nucleated bubble starts growing.

Assuming as initial conditions that the fluid velocity vanishes everywhere and that the temperature is constant and equal to T_f, we still have to decide the shape and size of the initial bubble. These variables have some significance during the early stages of bubble evolution, since they affect the initial shape of the shock front and also its initial acceleration. In $1+1$ dimensions it is possible to analytically find the extremum bubble of the effective action by solving the equation $\phi''(x) = \partial_\phi V(\phi, T_f)$. With $M^2 \equiv \gamma(T_f^2 - T_0^2)$, $\delta \equiv \alpha T_f$ and $\bar{\lambda} \equiv 9\lambda M^2/2\delta^2$ the solution is

$$\phi(x) = \frac{2\delta}{3\lambda}\,\frac{1-\sqrt{1-f(x)}}{f(x)}\,\bar{\lambda}, \tag{20}$$

where $f(x) \equiv (1-\bar{\lambda}\coth^2 Mx)/(1-\coth^2 Mx)$. A bubble obtained from this by increasing both the amplitude and radius by a small factor (by 5%) was normally used as the initial configuration. We experimented also with the exact extremum bubble and with a bubble smaller than this one. The exact extremum bubble did not evolve anywhere and the subcritical bubble collapsed, leaving behind a disturbance in the temperature and flow velocity propagating outward with sound velocity. This disturbance is caused by the fact that matter has to flow inward to fill in the area of lower energy density from where the subcritical bubble has disappeared.

4.2 Numerical results

In fig. 7 the initial stages of bubble formation are shown for the **qh** parameters. Immediately after the nucleation, a shock front is originated which spreads out information about the nucleation. At first the shock front is not sharp. The temperature starts to rise inside the bubble and very soon the phase transition front begins to get shape. At about the moment $t = 100(1/T_c)$, both the phase transition front and the shock front are clearly visible.

To get a more precise picture of the phase transition surface, we can use eqs. (11–13). (The solution of these eqs. is discussed in Section (5)). In fig. 8 the order parameter $\phi(x)$, the temperature $T(x)$, the velocity $v(x)$ and the quantity $\partial_T V$ are shown in the rest frame of the phase transition surface. Hadron phase is on the left and quark phase on the right. The width of the surface layer is a few correlation lengths. The curves resemble the $\tanh(x)$-function but for some other parameters the resemblance is not as clear. Specifically, the temperature and velocity distributions lose their symmetry and are shallower on the hadron side where the effective potential $V(\phi, T)$ is non-zero. The "center points" of these distributions are not quite at the

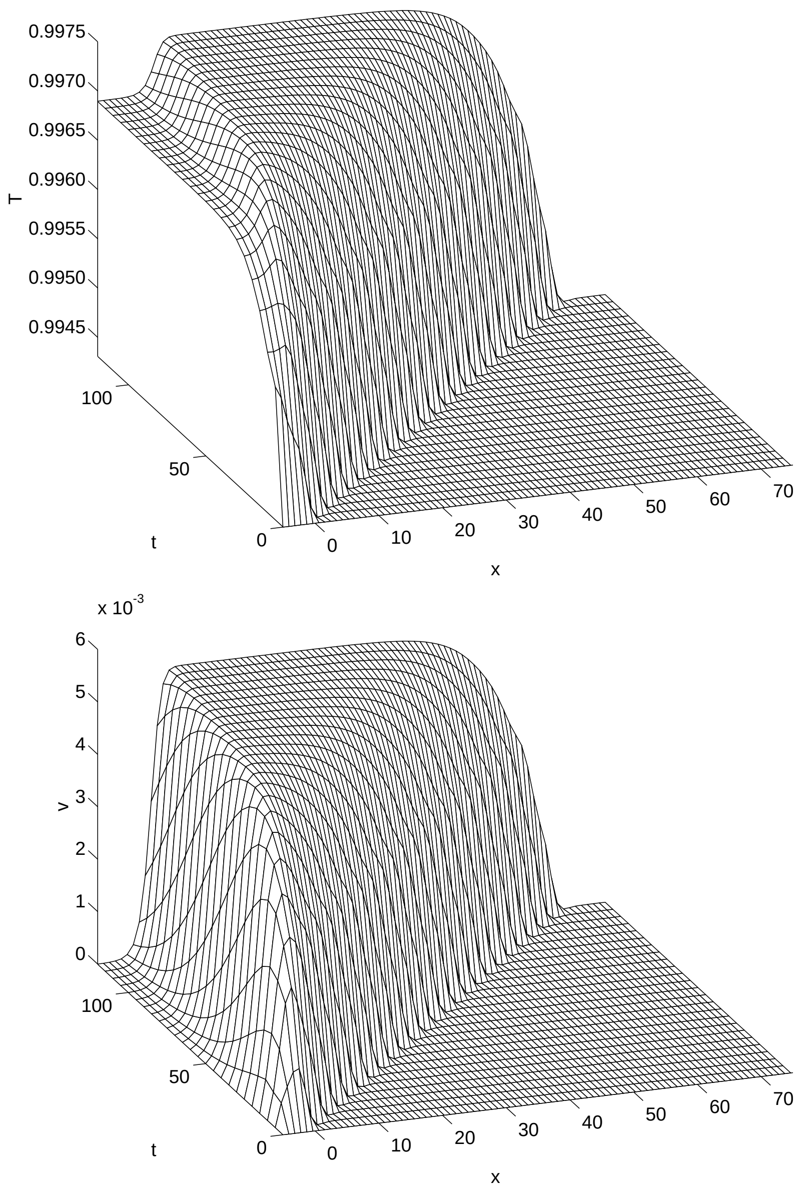

Fig. 7: The early stages of bubble growth. The upper picture shows $T(t,x)$ and the lower picture shows $v(t,x)$ for the **qh** parameters.

same place as that of the order parameter, but are shifted towards the hadron phase. For some parameters the shift can be of the order of ξ_c.

In fig. 9 the development of the shock front is illustrated. The shock front is shown at times $t = 160$ and $t = 3840$. At early times, the shape of the initial configuration strongly affects the shape of the shock front. However, after some time the shock front sharpens to a discontinuity [8] irrespective of its initial shape. To understand the physical reason for this, consider yourself moving with the shock front

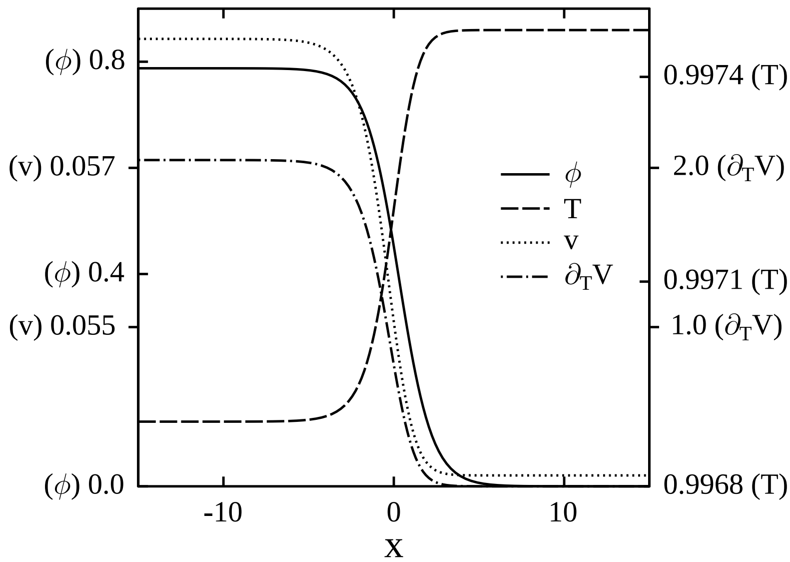

Fig. 8: The variables $\phi(x)$, $T(x)$, $v(x)$ and $\partial V/\partial T$ as measured in the rest frame of the stationary phase transition surface. Hadron phase is on the left and quark phase on the right. By the velocity v we denote here the absolute value of the velocity: the direction of flow is from the quark to the hadron phase.

and looking back towards the heated quark matter. Particles farther away from the front recede more slowly than particles just at the front. When the shock front is still smooth, it follows from energy-momentum conservation that entropy is conserved, i.e., with the quark matter equation of state,

$$\partial_t(T^3\gamma) + \partial_x(T^3\gamma v) = 0 \ . \tag{21}$$

This means that the temperature has to rise farther away from the front in order to accommodate the entropy of the matter moving with a lower velocity. However, as another consequence of energy-momentum conservation, temperature cannot rise enough to accommodate all the entropy inside a constant-sized volume, and a "traffic jam" -phenomenon occurs causing a discontinuity. An upper limit to the rate of jamming is clearly given by the difference of the velocity of the matter going into the jam and the velocity of the jam. This difference is just v_{fluid}. Then the time scale of the sharpening is determined by v_{fluid} and on how smooth the shock front was in the beginning. The latter depends on how near the initial configuration was of the extremum bubble. Because the shock front can initially be very wide and the flow velocity is very small, the time scale of the sharpening is very large.

In fig. 10 a collision of two bubbles is shown. Due to the use of reflective boundary conditions, our grid corresponds to a situation in which several bubbles nucleate simultaneously at equal spacings, and therefore collisions are possible. The

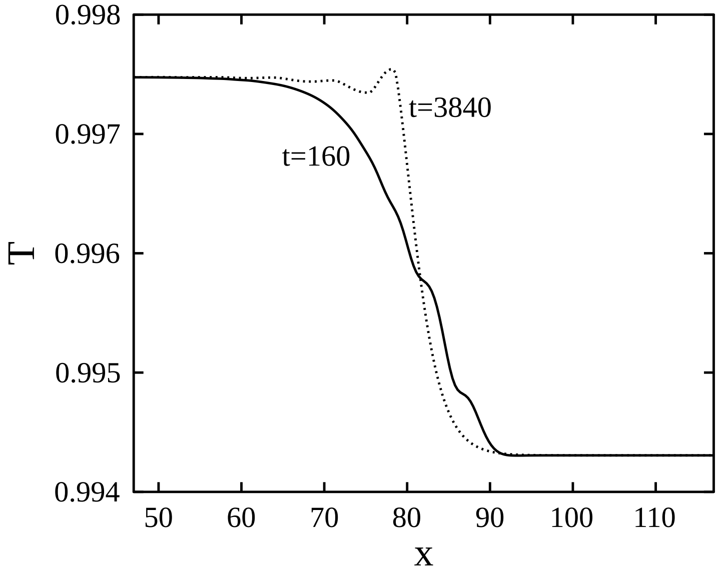

Fig. 9: The sharpening of the shock front.

distance between the bubbles is in our picture $\Delta x = 640$ which is much less than the actual distances in the early universe, but this is not essential for the present analysis. At time $t = 240$, both the phase transition surface and the shock front are moving to the right. At $t = 720$, the shock fronts of neighbouring bubbles have collided, and the quark matter between the reflected shocks heats to a temperature higher than T_c. At $t = 960$ the shock front and the phase transition surface are just about to collide; at $t = 1040$, the collision has just happened. The temperature of the hadron phase increases significantly. A shock front (a) continues to the hadron phase heating it up and making the matter move, but at the same time a rarefaction wave (b) is reflected back to the quark phase, cooling it down. The phase transition surface continues to move to the right, but its velocity has decreased from 0.06 to about 0.015. Some simple scenarios for the collision of a shock front and a deflagration front have been presented in ref. [9], and the course of events in fig. 10 is a combination of the scenarios **a** and **c**.

As was seen in fig. 10, even one shock front can heat the hadronic matter considerably. This implies that only a few shock fronts are needed to raise the temperature of the hadronic matter to T_c. This situation is shown in fig. 11, where several collisions are allowed to happen. The upper picture shows $T(t,x)$ and the lower picture $\phi(t,x)$. As the temperature of the hadron matter rises to T_c the growth of the hadron bubbles is halted. In the cosmological context, a stage of slow growth of the hadron bubbles along with the expansion of the universe follows. In the electroweak case, the latent heat is smaller and the critical temperature is not reached. The bubbles fill the space and the fluid reaches the reheating temperature $T_{\rm reheat}$.

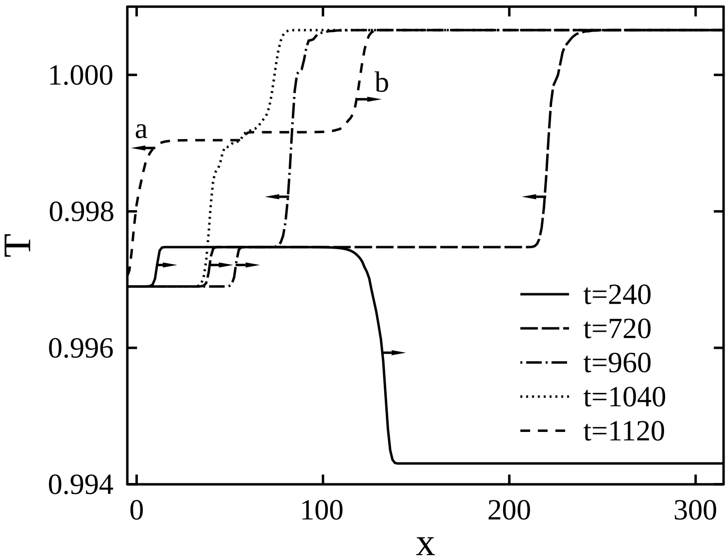

Fig. 10: The collision of two bubbles. See the body of text for explanation.

However, we must remember that the present simulations are 1+1 dimensional. In the 3-d case, the shock fronts are considerably weaker [8] and the time it takes for the universe to reheat is not necessarily the same as in the 1-d case. Neglecting the expansion of the universe, the fraction of space taken by the hadron matter immediately after reheating in the QCD case and the reheating temperature in the EW case are nevertheless the same as in the 1-d case.

All the numerical solutions we have discussed so far were deflagrations. However, using a larger supercooling than eq. (18) indicates for the above (**qh**) values of σ and L, we found detonation solutions. For $T_f = 0.90$ such a solution is shown in fig. 12. The upper picture shows $T(t,x)$ and the lower picture $\phi(t,x)$. The detonation expands with velocity $v_{\rm det} = 0.90$ and a rarefaction front follows slightly behind. This is a weak detonation.

As was seen in fig. 5, for some values of σ and L even the physical nucleation temperature is so low that detonations could appear. In particular, even though the latent heat L is usually taken to be of the order of T_c^4, there is nothing in the lattice computations to rule out the possibility that L could as well be $0.1T_c^4$ or even less. Using the parameter values[2] $\sigma = 0.1$, $L = 0.1$, and $\xi_c = 6$, we did a sequence of computer runs varying the value of Γ (see fig. 13). This results in considerable supercooling, and the nucleation temperature (eq. (18)) is $T_f = 0.891T_c$. For small values of Γ the bubbles grow as weak deflagrations. Increasing Γ increases $v_{\rm def}$, until at about $\Gamma = 10$ it approaches c_s. Now $v_{\rm def} > c_s$ would indicate a strong deflagration.

[2]The larger value of ξ_c is needed for the potential of eq. (1) to be applicable for the range of temperatures in question.

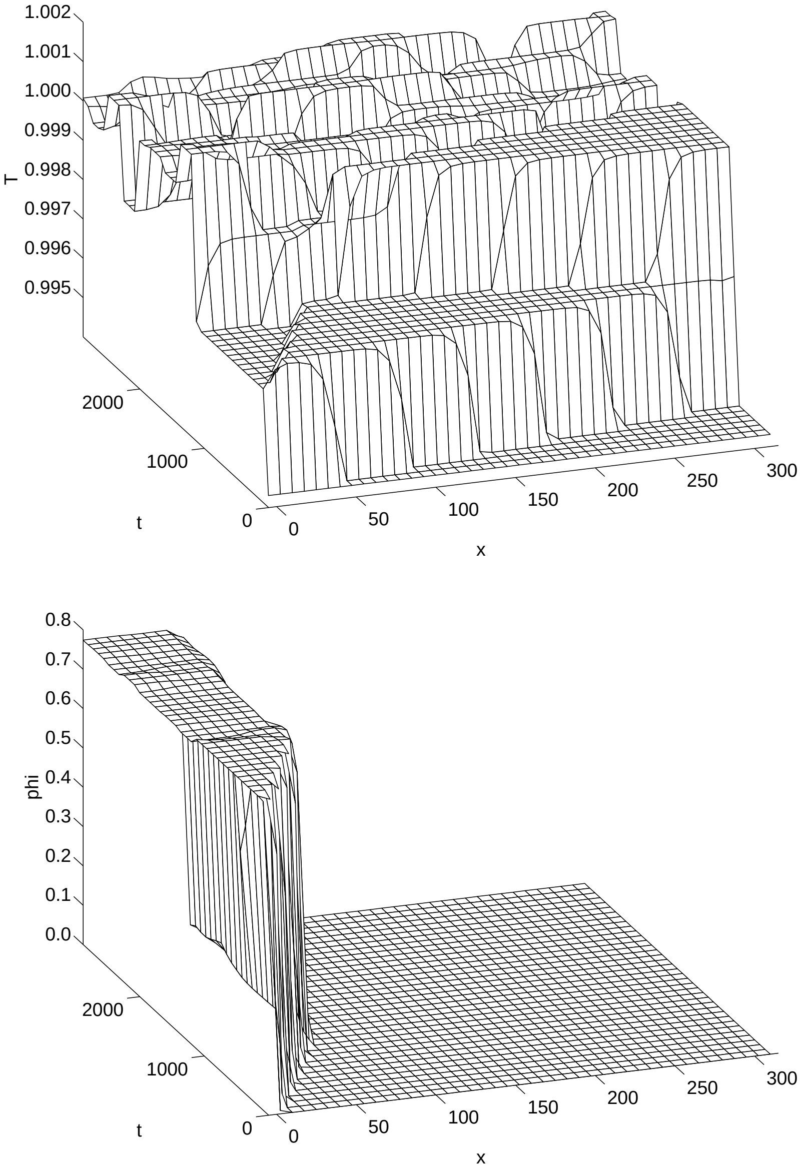

Fig. 11: Final stages of the phase transition for the **qh** parameters.

Instead, as Γ is further increased, the solution shifts to a weak detonation.

5 Steady-state variables of deflagration bubbles

Very soon after the nucleation, the growing bubbles reach a steady-state configuration (see fig. 7). In the steady-state situation there exists a simple and very accurate way of finding out the interesting stationary variables T_q, T_h, $v_{\rm shock}$, $v_{\rm fluid}$ and $v_{\rm def}$ of the deflagration bubble apart from the above-presented integration of eqs. (9).

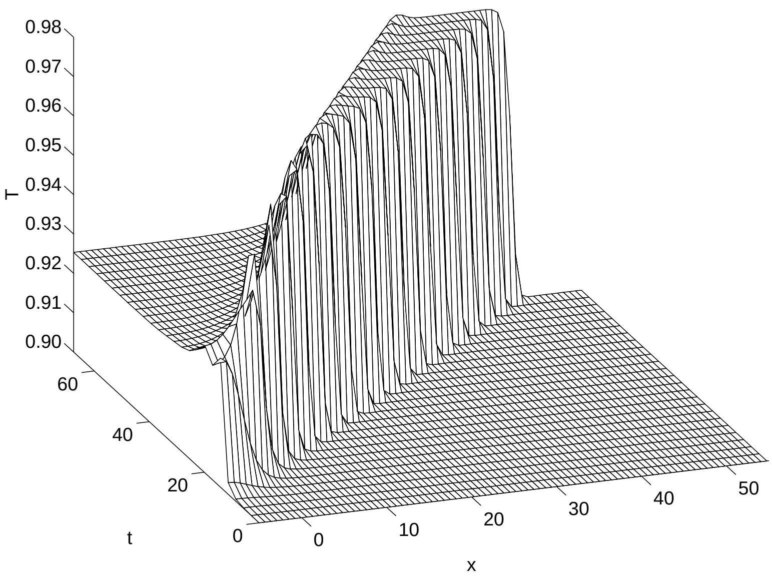

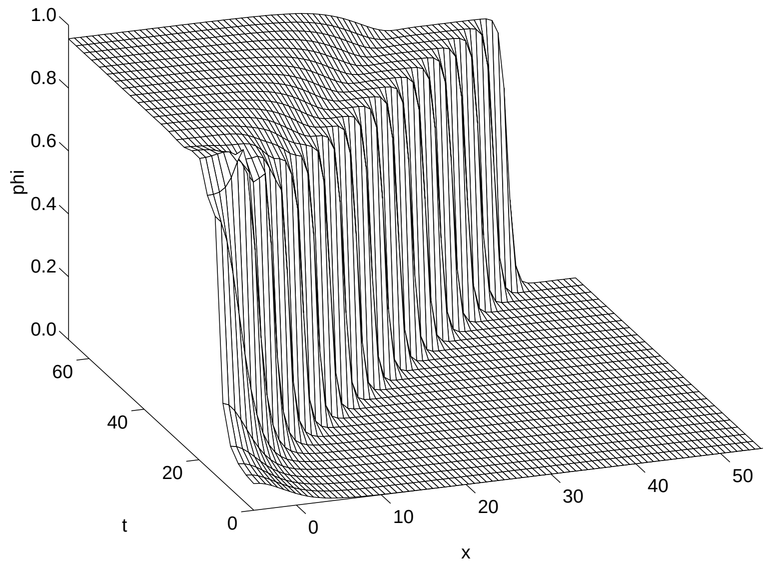

Fig. 12: A detonation solution for the **qh** parameters with $\Gamma = 2$ and $T_f = 0.90$. Note that $\phi_{\rm min}$ depends on temperature.

This method can also be used to check the accuracy of the above integration. In the rest frame of the phase transition front the equations to be solved were given in eqs. (11–13).

Let us think that with the two conservation equations (12) and (13), we solve for $T(x)$ and $v(x)$ in terms of $\phi(x)$ and $\phi'(x)$. Substituting these to eq. (11), we get a second order differential equation for the field ϕ alone. However there are *three* boundary conditions: the derivative $\phi'(x)$ must vanish asymptotically in both phases

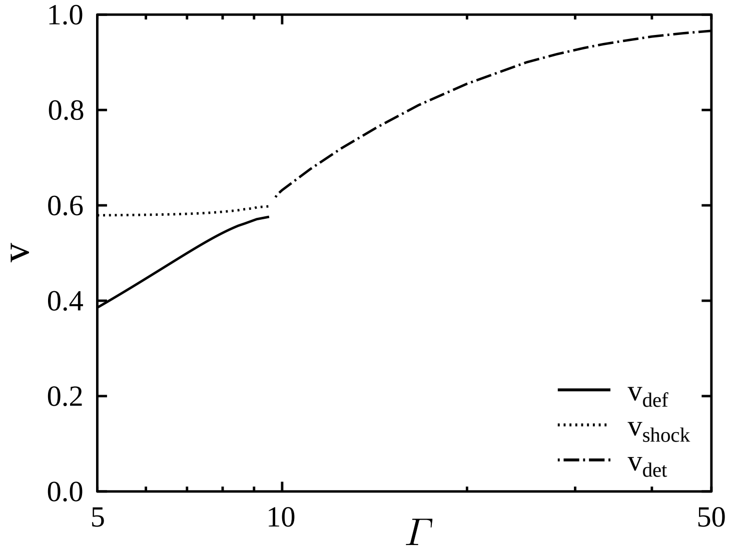

Fig. 13: The bubble growth velocity for $\sigma = 0.1$, $L = 0.1$ and $\xi_c = 6$ as a function of the parameter Γ. At approximately $\Gamma = 10$ the solution changes from a weak deflagration to a weak detonation.

and we know the value of the field $\phi(x)$ (only) in the quark phase. The system is overdetermined, and only for certain values of the "constants" are there solutions. This is thus an eigenvalue problem. Assuming that we are given T_q, we can solve for T_h, $v_{\rm def}$ and $v_{\rm fluid}$.

Next, consider the shock front. Because the shock front is in the quark phase, the field ϕ vanishes everywhere and we are left with very simple energy-momentum conservation equations. Solving them [4, §135] we get

$$\begin{aligned} v_1 &= \tfrac{1}{\sqrt{3}}\sqrt{\tfrac{3T_q^4+T_f^4}{3T_f^4+T_q^4}} \\ v_2 &= \tfrac{1}{3v_1}. \end{aligned} \tag{22}$$

Therefore, given T_f and T_q, we can write down $v_{\rm shock} = v_1$ and $v_{\rm fluid} = (3/2)(v_1 - v_2)$.

Now remember that *a priori* we only know T_f. However, guessing some T_q, we get both from eqs. (11–13) and eq. (22) a value for $v_{\rm fluid}$. When we manage to guess such a T_q that these two numbers agree the whole problem is solved. It is easy to make this method of solving the steady-state variables very accurate. Therefore we can use this method to check the accuracy of the dynamical integration with all time derivatives. With a reasonable number of grid points, the differences between the results of the two methods of integration on the steady-state variables are much less than 1% . Using this method, we can also easily calculate the steady-state variables as a function of Γ.

5.1 Analytical approximations

In this section we study what can be said analytically of the solutions of the steady-state equations (11–13). We use the bag equation of state (16,17) and assume that the velocities v_q and v_h are non-relativistic ($v^2 \ll 1$) and that the temperatures T_q and T_h are near T_c ($T_q - T_h \ll T_c$). The entropies are $s_q = 4a_qT_q^3$ and $s_h = 4a_hT_h^3$ and the enthalpy is $w = Ts$. The one-parameter family of solutions of the two equations (12) and (13) has been studied in detail in the literature [7,8,9,12,15,18], and the main problem is to find which solution the new equation (11) picks out of this family.

Evaluating eqs. (12) and (13) in the rest frame of the phase transition front for $x = -\infty$ and $x = \infty$ one obtains the usual energy-momentum conservation equations

$$\begin{aligned} w_qv_q &= w_hv_h \\ w_qv_q^2 + p_q &= w_hv_h^2 + p_h \ . \end{aligned} \tag{23}$$

From the upper equation it follows that

$$\frac{v_h}{v_q} = \frac{w_q}{w_h} = \frac{a_qT_q^3}{a_hT_h^3} \approx \frac{a_q}{a_h} \equiv r \ . \tag{24}$$

Thus the fluid velocity is related to the deflagration front velocity by

$$v_{\text{fluid}} = v_h - v_q = (1 - 1/r)v_{\text{def}} \ . \tag{25}$$

From the lower of eqs. (23) we get

$$v_qv_h = rv_q^2 = \frac{p_h - p_q}{w_h - w_q} = \frac{a_hT_h^4 + L/4 - a_qT_q^4}{4a_hT_h^4 - 4a_qT_q^4} \tag{26}$$

which in the limit $T_q, T_h \approx T_c \equiv 1$ implies that

$$1 - T_h = r(1 - T_q) + r(r-1)v_q^2 \ . \tag{27}$$

To find the consequences of eq. (11), multiply it by $\phi'(x)$ and integrate over the real axis. Using the equations $\partial V(\phi, T)/\partial\phi = dV/d\phi - (\partial V/\partial T)(dT/d\phi)$, $V(-\infty) = -L(1 - T_h)$, $V(\infty) = 0$ and $\phi'(\pm\infty) = 0$, and replacing the velocity $v(x)$ by its absolute value (see fig. 8) one obtains

$$L(1 - T_h) = \frac{1}{\Gamma}\int_{-\infty}^{\infty} [\phi'(x)]^2 v(x)\, dx - \int_{T_q}^{T_h} \frac{\partial V}{\partial T} dT \ . \tag{28}$$

This is easy to solve in the limit $r = v_h/v_q \to 1$ and $T_h, T_q \to T_c$ since then one can take $v(x) \approx v_h \approx v_q$ out of the first integral (which then gives the interface tension σ) and neglect the last term. The result is

$$v_h \approx v_q \approx v_b \equiv \Gamma\frac{L}{\sigma}(1 - T_q). \tag{29}$$

This is the formula for bubble wall velocity derived earlier [11,14,15,16] for the case of small change in flow velocity, which may be appropriate for the EW phase transition.

In the more general case $r > 1$ note first that, because $\phi'(x)$ is approximately symmetric around $x = 0$, the first term in eq. (28) can be approximated by $(\sigma/\Gamma)\cdot(v_q + v_h)/2$. From fig. 8 one sees that at $x = 0$, $\partial V/\partial T$ is about $L/2$ (in the hadron phase, $\partial V/\partial T \approx L$, since $V(-\infty) \approx -L(1-T_h)$, see above). We therefore approximate the second term by $-\kappa(L/2)(T_h - T_q)$, where κ is of order unity. Using eqs. (24) and (27), eq. (28) then becomes

$$(1-\frac{\kappa}{2})Lr(r-1)v_q^2 - \frac{\sigma(r+1)}{2\Gamma}v_q + L(1-T_q)[r+\frac{\kappa}{2}(1-r)] = 0 \ . \tag{30}$$

From this one can solve $v_{\rm def} = v_h = rv_q$ as a function of T_q. If further $\kappa = 1$, eq. (30) simplifies into the form

$$\left(\frac{r-1}{r+1}\right)v_{\rm def}^2 - \frac{\sigma}{L\Gamma}v_{\rm def} + r(1-T_q) = 0 \ , \tag{31}$$

which for small Γ (small $v_{\rm def}$) again gives the result $v_q = v_b$ in eq. (29).

It is worth noticing that from eq. (30) we get a lower bound for T_q. Namely, we know that eq. (30) has a solution and this gives

$$T_q \geq 1 - \frac{\sigma^2(r+1)^2}{16L^2\Gamma^2 r(r-1)(1-\kappa/2)[r+(\kappa/2)(1-r)]} \ . \tag{32}$$

The numerical value of this formula is useful for large Γ. However, even for moderate Γ it is essential to notice the *existence* of a lower bound: the temperature T_q is not a free physical parameter, and when the whole expanding physical bubble is considered, the shock wave always heats quark matter just enough to reach the safe T_q area.

To obtain the result for a true deflagration bubble one finally has to eliminate the temperature T_q from eq. (31) by using eq. (22). Expanding $v_{\rm fluid}$ in powers of $1-T_q$ and $1-T_f$ one gets

$$v_{\rm fluid} = \sqrt{3}\,[(1-T_f)-(1-T_q)] \ . \tag{33}$$

Using eq. (25) and substituting $1-T_q$ in terms of $v_{\rm def}$ into eq. (31) gives

$$\left(\frac{r-1}{r+1}\right)v_{\rm def}^2 - \left(\frac{\sigma}{L\Gamma}+\frac{r-1}{\sqrt{3}}\right)v_{\rm def} + r(1-T_f) = 0 \ . \tag{34}$$

From this the final equation for $v_{\rm def}$ as a function of Γ is

$$v_{\rm def} = \left[\frac{\sigma}{L\Gamma}+\frac{r-1}{\sqrt{3}} - \sqrt{\left(\frac{\sigma}{L\Gamma}+\frac{r-1}{\sqrt{3}}\right)^2 - 4r(1-T_f)\left(\frac{r-1}{r+1}\right)}\,\right] \Big/ 2\left(\frac{r-1}{r+1}\right) \ . \tag{35}$$

This is an excellent approximation for non-relativistic deflagration front velocities as will be seen in the next section (see fig. 15). In the limit $\Gamma \to 0$ eq. (35) correctly reduces to the further approximation $v_{\rm def} \approx r\Gamma(L/\sigma)(1-T_f)$.

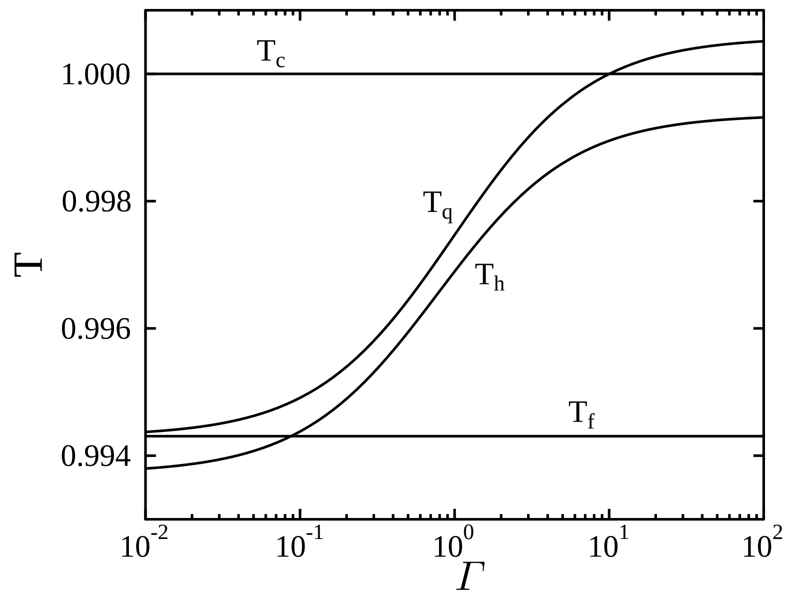

Fig. 14: The temperatures T_f, T_c, T_q, T_h as a function of Γ for the **qh** parameters.

5.2 Numerical results for steady-state walls

5.2.1 The quark-hadron phase transition

In fig. 14 the temperatures T_f, T_q and T_h are shown as a function of Γ for **qh** parameters. Small Γ means large friction and small velocities; large Γ means small friction and large velocities. When the deflagration front velocity is small, equation (25) tells us that the fluid velocity is very small (for our present parameters, $r \approx 1.1$ so that $v_{\mathrm{fluid}} \approx 0.1 v_{\mathrm{def}}$). Then from eqs. (22) we learn that T_q has to be very close to T_f. For large Γ the situation is opposite: the velocities are larger and T_q is higher. The temperatures T_q and T_h satisfy the relation (27) very accurately. Notice that entropy production at the shock front requires the condition $T_q > T_f$ and obviously one also has to obey the condition $T_h < T_c$, but nothing prevents T_q from exceeding T_c. This fact has been noticed before (see e.g. ref. [7]), but usually it is not taken seriously. One reason may be that some authors neglect proper boundary conditions and thus confuse T_q with T_f. Another is that it has been argued in refs. [44,45] that a transition front between quark matter at the temperature $T_q > T_c$ and hadron matter at the temperature $T_h < T_c$ is impossible, basically because such a front would be mechanically unstable. However, both arguments are based on the assumption that at T_c there exists a homogeneous mixed phase, and that in the transition zone between the quark phase and the hadron phase, the state of the matter is at some point just in this homogeneous mixed phase. Then the transition front would be equal to two transition fronts, one from the quark phase to the mixed phase and the other from

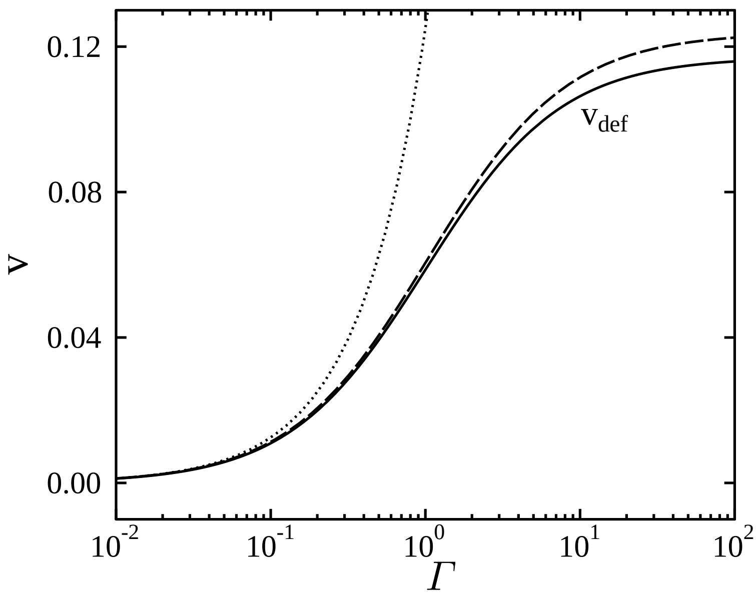

Fig. 15: The velocity $v_{\rm def}$ as a function of Γ for the **qh** parameters. The dashed line is the approximation from eq. (35) and the dotted line is the further approximation $v_{\rm def} \approx r\Gamma(L/\sigma)(1-T_f)$.

the mixed phase to the hadron phase. If there is a microscopic order parameter field — like in our model — the order parameter interpolates between the two minima of the effective potential in the transition zone, and there is no homogeneous mixed phase. The only mechanism by which a phase transition surface of this kind could in principle split is that a rarefaction wave detaches from it, and the analysis in ref. [45] does not apply to rarefaction waves. Hence, there seems to be no reason why T_q could not exceed T_c, if the phase transition effectively includes an order parameter field.

In fig. 15 the propagation velocity of the phase transition surface $v_{\rm def}$ is shown with solid line. With the dashed line we have drawn the deflagration front velocity from eq. (35). This equation is seen to hold very well when the velocity $v_{\rm def}$ is non-relativistic. The simple small-velocity approximation $v_{\rm def} \approx r\Gamma(L/\sigma)(1-T_f)$ is drawn with dotted line. In fig. 16 the fluid velocity $v_{\rm fluid}$ is shown as a function of Γ (solid line) and in fig. 17 the shock velocity $v_{\rm shock}$ is drawn (solid line). The shock velocity is compared to the sound velocity.

In fig. 16, the dotted line shows the entropy production. By entropy production we mean the relative change of the total entropy of a fluid element as the shock front and the phase transition surface sweep over it. One must note that the volume of the

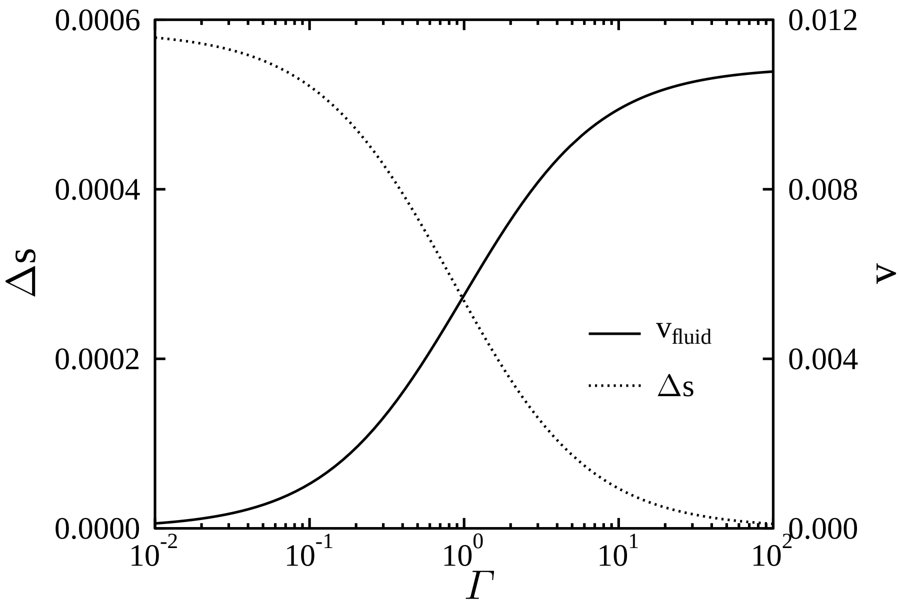

Fig. 16: The fluid velocity and the entropy production for the **qh** parameters.

fluid element changes in the course of the process by the relative amount (see fig. 18)

$$\rho_V = \frac{V_{\text{final}}}{V_{\text{initial}}} = \frac{1 - v_{\text{fluid}}/v_{\text{shock}}}{1 - v_{\text{fluid}}/v_{\text{def}}} > 1 \ . \tag{36}$$

Therefore we define the entropy production by

$$\Delta s \equiv \frac{s_h(T_h)\rho_V - s_q(T_f)}{s_q(T_f)} \ . \tag{37}$$

In the quark-hadron phase transition where there is a conserved baryon number, this is just the relative change of entropy per baryon. The entropy production in eq. (37) is related to the quantity $\Delta s_{\text{pw}} \equiv s_h \gamma_h v_h - s_q \gamma_q v_q$ (measured in the rest frame of the phase transition surface), which is often (e.g. in ref. [12]) used to describe entropy production, and to the analogously defined quantity Δs_{sh} measured in the rest frame of the shock front, by the equation

$$\Delta s = \left(\frac{\Delta s_{\text{sh}}}{\gamma_{\text{sh}} v_{\text{sh}}} + \frac{\Delta s_{\text{pw}}}{\gamma_{\text{def}} v_{\text{def}}} \rho_V \right) / s_q(T_f) \ . \tag{38}$$

The first term in the numerator is vanishingly small in comparison to the second.

According to ref. [18] the quantity $\eta \equiv -T_c(dv_{\text{def}}/dT_q)v_{\text{def}}$ determines the stability of expanding bubbles. If $\eta > 1$, the bubbles are stable at all length scales; if $\eta < 1$, large scale fluctuations are unstable. For our **qh** parameters, the quantity η is drawn in fig. 17 with dotted line. While the analysis of ref. [18] is not suited for large Γ where T_q can exceed T_c, we notice, however, that for $\Gamma < 0.83$ our numerical

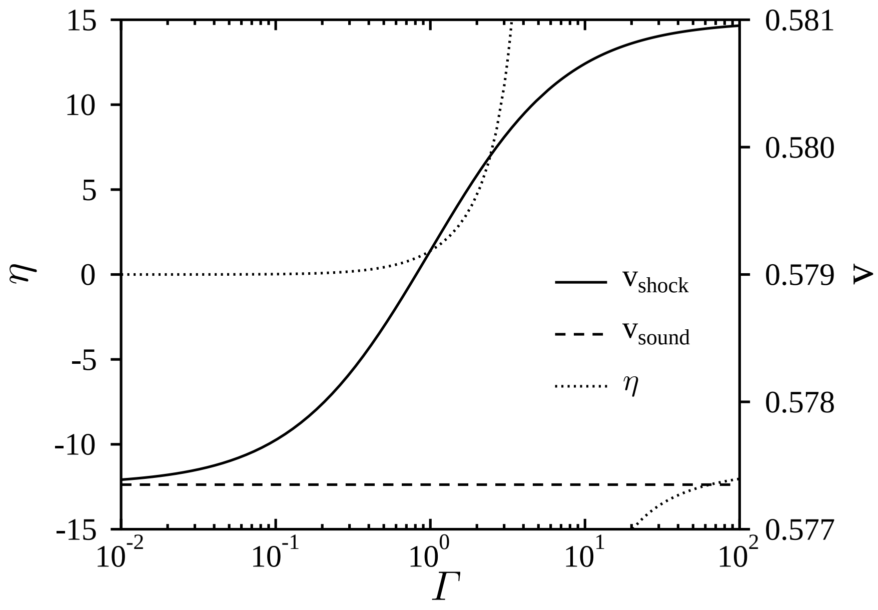

Fig. 17: The shock velocity and the parameter η for the **qh** parameters.

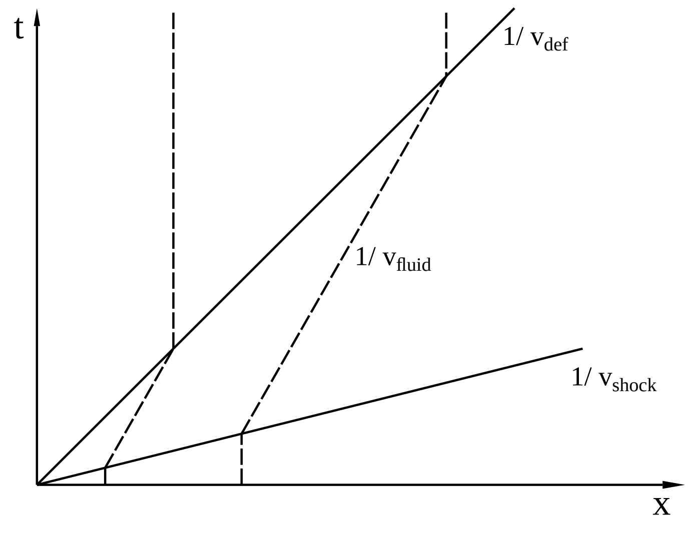

Fig. 18: The dashed lines indicate the average fluid flow in a similarity deflagration solution. The volume of a fluid element changes when the shock front and the deflagration front sweep over it.

results imply η to be less than unity and therefore large scale fluctuations should be unstable in that case. It would be interesting to expand the present code to include more space dimensions to see whether the expanding bubbles remain stable.

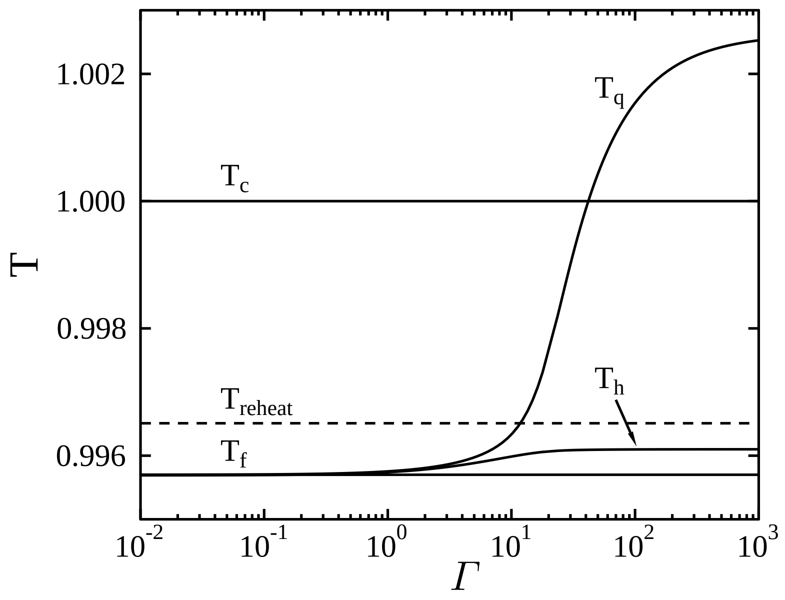

Fig. 19: The temperatures T_f, T_c, T_q, T_h and $T_{\rm reheat}$ for the **ew** parameters.

5.2.2 The electroweak phase transition

In figs. 19–20 we address the same questions as above but for the **ew** parameters. Qualitatively the behaviour is rather similar to what it was for the **qh** case. However, some differences worth a comment exist. The most important difference is that the electroweak phase transition is essentially a massless transition: the number of effective degrees of freedom changes very little at T_c. Quantitatively this is expressed by the fact that $r = a/(a - L/4) = 1.0018$ is much closer to unity than in the **qh** case. Because of the smallness of r, there is a new temperature relevant for the phase transition. This is the reheating temperature $T_{\rm reheat}$ (in the abrupt reheating scenario), defined by the equation $\epsilon_q(T_f) = \epsilon_h(T_{\rm reheat})$. For our present **ew** parameters, $T_{\rm reheat} = 0.9965$.

Consider the temperatures (fig. 19) and the deflagration front velocity (fig. 20). Because the energy liberated in the phase transition is travelling in the compressed region behind the shock front, the temperature T_h can never reach $T_{\rm reheat}$. This keeps T_h low even for large Γ. On the other hand, it follows from eq. (35) that for large Γ the velocities $v_{\rm def}$ and $v_{\rm fluid}$ grow large (now $v_{\rm fluid} \approx 0.002 v_{\rm def}$). Then it is seen from eqs. (22) that the temperature T_q has to rise considerably when Γ is large. But with r close to unity and the difference between T_q and T_h large, it is seen from eq. (27) that the deflagration front velocity has to be very large indeed for large Γ. In fact the velocity $v_{\rm def}$ becomes moderately relativistic and eqs. (23–35) are no longer strictly applicable. Another way to understand the connection between the high temperature

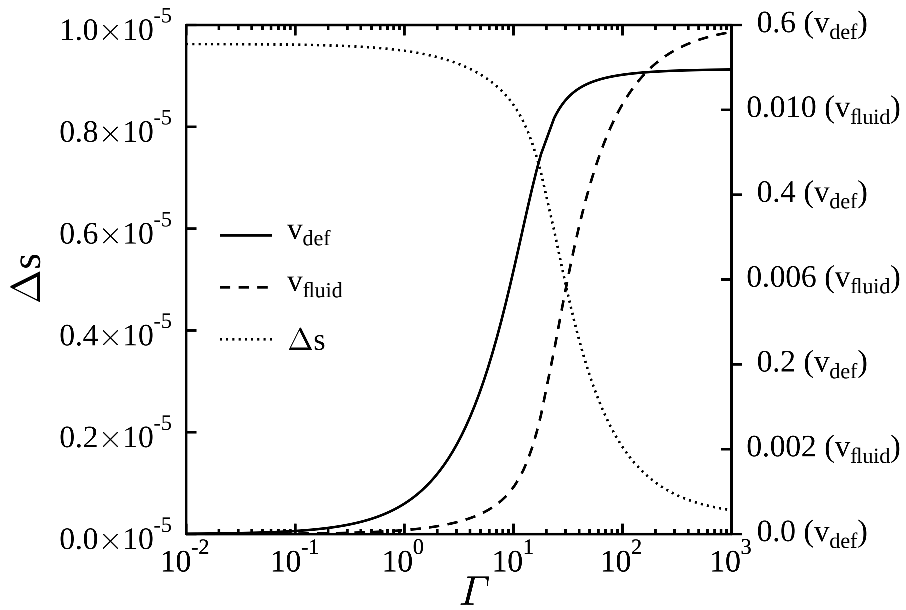

Fig. 20: The deflagration front velocity, the fluid velocity and the entropy production for the **ew** parameters.

T_q and the large velocity $v_{\rm def}$ is to notice that the closer $v_{\rm def}$ is to the shock front velocity, the thinner is the area between the shock front and the phase transition surface. Therefore this thin area has a high temperature in order to accommodate all the latent heat released.

Comparing figs. 14 and 19 we notice that for the **ew** parameters the values of Γ where $v_{\rm def}$ changes rapidly are larger than for the **qh** case. From eq. (35) we see that the relevant scale for Γ is roughly $\sigma(r+1)/L(r-1)$. For the **qh** case the numerical value of this quantity is 1.1 and for the **ew** case 96 which explains the difference.

Finally, let us compare our results to those of some other authors. Recently, the velocity of growing deflagration bubbles in the EW phase transition has been estimated for instance in refs. [14,16]. In ref. [16] the authors note that the relation $v_{\rm def} > 1/30$ has to be satisfied in order not to diffuse away the baryon asymmetry and that probably $\gamma v \approx 1-2$, that is, $v \approx 0.7-0.9$. This corresponds to strong deflagrations, which seem to be an unlikely mechanism for bubble growth [4,5]. In ref. [14] velocities of order $0.1-0.2$ are obtained. Using simple kinetic theory to estimate the value of Γ we get $\Gamma \approx 10-100$ [11,34], and then from fig. 20 mildly relativistic velocities appear to be very natural.

6 Conclusions

We have presented a model for phase transition bubbles in the early universe. In our model an order parameter field ϕ with an effective potential $V(\phi, T)$ is coupled to a fluid with a dissipative constant Γ. Starting from an initial condition of a newly nucleated bubble we have numerically evolved the coupled hydrodynamical and field equations to follow the growth of the bubble in 1+1 dimensions. After some time the bubble reaches a stationary (similarity) state, where it grows at a constant velocity. We have then also studied the solutions to the corresponding stationary equations, both numerically and in analytical approximations.

Typically the bubbles grow as weak deflagrations, and therefore with a subsonic velocity. The growth velocity is determined by the value of Γ, a large Γ (a weak coupling between ϕ and the fluid) leading to a large velocity and vice versa. Thus, we have been able to reduce the calculation of the growth velocity to the microscopic calculation of Γ. Our results show that the preheating caused by the shock front plays an essential role in the growth process, and that the temperature T_q could even exceed T_c. Reheating caused by collisions of expanding bubbles was also explicitly computed.

If one uses simple kinetic theory to estimate Γ for the EW transition, one is naturally led to mildly relativistic velocities. For the QCD transition, one would dimensionally expect that $\Gamma \approx 1$ [15]. Then from fig. 15 for $L = 2T_c^4$, $\sigma = 0.1T_c^3$ we note that $v_{\rm def} \approx 0.06$. The expectation thus is that the velocities in the QCD case are smaller than in the EW case.

In some regions of the parameter space the solutions switch from weak deflagrations to weak *detonations*, as Γ is increased. It has been speculated that instabilities could turn expanding deflagration bubbles into detonations [17]. We have now found that in some cases the bubbles could expand as detonations even from the beginning. Often it has been assumed that detonations in these phase transitions would have to be Jouguet detonations [6,7], as in chemical burning [4,5], but this appears not to be the case [46]. In the cosmological context, weak detonations require less extreme conditions than Jouguet detonations, making detonations more likely.

For the QCD phase transition, there is an interesting parameter region that cannot presently be ruled out. Here the latent heat is rather small, say $L = 0.1T_c^4$, and the surface tension is similar, say $\sigma = 0.1T_c^3$. Then the average distance between the nucleation centers would be of the order of 10 meters and large scale hadronic inhomogeneities would result. With our model we find that such bubbles could grow as detonations, leading to a picture of the phase transition that is rather different from the usual one.

Acknowledgements

We thank the Academy of Finland for financial support, K. Rummukainen and P. V. Ruuskanen for discussions and the Finnish Center For Scientific Computing for computational facilities.

References

[1] S. Coleman, Phys. Rev. D15 (1977) 2929;
C. Callan and S. Coleman, Phys. Rev. D16 (1977) 1762

[2] A. Linde, Phys. Lett. B70 (1977) 306, B100 (1981) 37

[3] A. Linde, Nucl. Phys. B216 (1983) 421

[4] L. D. Landau and E. M. Lifshitz, *Fluid Mechanics*, 2nd edition (Pergamon Press, Oxford, 1987)

[5] R. Courant and K. O. Friedrichs, *Supersonic flow and shock waves* (Springer-Verlag, Berlin, 1985)

[6] P. J. Steinhardt, Phys. Rev. D25 (1982) 2074

[7] M. Gyulassy, K. Kajantie, H. Kurki-Suonio and L. McLerran, Nucl. Phys. B237 (1984) 477

[8] H. Kurki-Suonio, Nucl. Phys. B255 (1985) 231

[9] K. Kajantie and H. Kurki-Suonio, Phys. Rev. D34 (1986) 1719

[10] J. S. Langer, in *Solids Far from Equilibrium*, pp. 297-363, ed. G. Godrèche (Cambridge University Press, 1992)

[11] N. Turok, Phys. Rev. Lett. 68 (1992) 1803

[12] K. Enqvist, J. Ignatius, K. Kajantie and K. Rummukainen, Phys. Rev. D45 (1992) 3415

[13] G. Anderson and L. Hall, Phys. Rev. D45 (1992) 2685

[14] M. Dine, R. G. Leigh, P. Huet, A. Linde and D. Linde, Phys. Rev. D46 (1992) 550

[15] K. Kajantie, Phys. Lett. B285 (1992) 331

[16] B. H. Liu, L. McLerran and N. Turok, Phys. Rev. D46 (1992) 2668

[17] M. Kamionkowski and K. Freese, Phys. Rev. Lett. 69 (1992) 2743

[18] P. Huet, K. Kajantie, R. G. Leigh, B. H. Liu and L. McLerran, Stanford Preprint SLAC-PUB-5943, to be published in Phys. Rev. D

[19] F. C. Adams, K. Freese and J. S. Langer, Phys. Rev. D47 (1993) 4303

[20] F. Karsch and E. Laermann, Bielefeld Preprint BI-TP 93-10, to be published in Rep. Prog. Phys.

[21] L. Dolan and R. Jackiw, Phys. Rev. D9 (1974) 3320

[22] M. Carrington, Phys. Rev. D45 (1992) 2933

[23] M. Shaposhnikov, Phys. Lett. B277 (1992) 324, B282 (1992) 483 (Erratum)

[24] C. G. Boyd, D. E. Brahm and S. Hsu, Caltech Preprint CALT-68-1795 (1992)

[25] P. Arnold and O. Espinosa, Phys. Rev. D47 (1993) 3546

[26] A. Hebecker, DESY Preprint DESY 93-086

[27] B. Bunk, E.-M. Ilgenfritz, J. Kripfganz and A. Schiller, Nucl. Phys. B403 (1993) 453

[28] K. Kajantie, K. Rummukainen and M. Shaposhnikov, CERN-TH.6901/93, to be published in Nucl. Phys. B

[29] K. Farakos, K. Kajantie, K. Rummukainen and M. Shaposhnikov, CERN-TH.6973/93

[30] A. Albrecht, P. J. Steinhardt, M. S. Turner and F. Wilczek, Phys. Rev. Lett. 48 (1982) 1437

[31] H. Kurki-Suonio, J. Centrella, R. A. Matzner, and J. R. Wilson, Phys. Rev. D35 (1987) 435

[32] S. Yu. Khlebnikov, Phys. Rev. D46 (1992) R3223

[33] P. Arnold, Phys. Rev. D48 (1993) 1539

[34] M. Carrington and J. Kapusta, Phys. Rev. D47 (1993) 5304

[35] J. C. Miller and O. Pantano, Phys. Rev. D42 (1990) 3334

[36] Y. Iwasaki *et al.* (QCDPAX Collaboration), Phys. Rev. D46 (1992) 4657

[37] B. Grossmann and M. L. Laursen, Jülich Preprint HLRZ-93-7

[38] Y. Iwasaki, K. Kanaya, L. Kärkkäinen, K. Rummukainen and T. Yoshié, CERN-TH.6798/93

[39] S. A. Bonometto and O. Pantano, Phys. Rep. 228 (1993) 175

[40] J. R. Wilson, in *Sources of Gravitational Radiation*, ed. L. L. Smarr (Cambridge University Press, 1979);
J. Centrella and J. R. Wilson, Astrophys. J. 273 (1983) 428,
Astrophys. J. Supp. 54 (1984) 229

[41] J. P. Boris and D. L. Book, J. Comp. Phys. 11 (1973) 38

[42] H. von Gersdorff, L. McLerran, M. Kataja and P. V. Ruuskanen, Phys. Rev. D34 (1986) 794

[43] L. D. Landau and E. M. Lifshitz, *Statistical Physics*, Part 1, 3rd edition (Pergamon Press, Oxford, 1988)

[44] P. Danielewicz and P. V. Ruuskanen, Phys. Rev. D35 (1987) 344

[45] M. I. Gorenstein and V. I. Zhdanov, Z. Phys. C34 (1987) 79

[46] M. Laine, Helsinki Preprint HU-TFT-93-44 (Bulletin Board: hep-ph/9309242)